Surface-Enhanced Raman Scattering for Redox-Active Adsorbates: Pentaammineosmium(III)/(II) and Pentaammineruthenium(II) Containing Nitrogen Heterocycle Ligands

Stuart Farquharson,[1a] Kendall L. Guyer,[1b] Peter A. Lay,[1c] Roy H. Magnuson,[1c] and Michael J. Weaver*[1a]

Contribution from the Department of Chemistry, Purdue University, West Lafayette, Indiana 47907, and the Department of Chemistry, Stanford University, Stanford, California 94305. *Received September 19, 1983*

Abstract: Surface-enhanced Raman scattering (SERS) for pentaammineosmium(III) and pentaammineruthenium(II) containing pyridine (py), pyrazine (pz), or 4,4′-bipyridine (bpy) ligands adsorbed at the silver–aqueous interface has been examined as a function of electrode potential to explore vibrational changes associated with electron transfer involving simple adsorbates. SERS was observed for the pyridine complexes despite their lack of an unshared electron pair for surface binding, although more intense spectra were obtained for the pyrazine and bipyridine complexes which contain a remote nitrogen lone pair. SER vibrational bands for metal–ligand and internal ammine modes were observed in addition to those due to heterocycle ring modes. Marked shifts were observed in the frequency of several vibrational bands for adsorbed $Os(NH_3)_5py$ and $Os(NH_3)_5pz$ as the electrode potential was made more negative that are consistent with the reduction of Os(III) to Os(II). The potential-dependent concentrations of adsorbed Os(III) and Os(II) as determined by using SERS are in good agreement with those obtained from rapid cyclic voltammetry. The bulk-phase Raman spectra exhibit resonance enhancement. Such electronic resonance also contributes to the overall signal enhancement seen in the SER spectra.

The recent discovery of surface-enhanced Raman scattering (SERS) for adsorbates at silver, copper, and gold surfaces has generated much experimental and theoretical activity aimed at understanding the underlying physical phenomena.[2] The SERS technique also holds promise as a major tool for investigating the detailed molecular properties of adsorbates in electrochemical environments, for which spectroscopic examination had previously been impractical.[2a,c] Although a variety of electrochemical adsorbates have now been demonstrated to yield SERS, surprisingly few attempts have been made to quantitatively relate the nature and intensity of SERS signals to the electrochemical properties of the system.

To this end, the Purdue group has been examining SERS of structurally simple adsorbates at silver–aqueous interfaces for which independent information can be obtained on the surface composition and structure.[3-5] In particular, we have demonstrated simple relationships between the intensity of SERS signals and the coverage for a number of simple anionic adsorbates as determined from corresponding capacitance–potential data.[3] Our overall objective is to utilize SERS not only to gain detailed information on structure and bonding for electrochemical adsorbates but also to follow molecular transformations, especially electron-transfer reactions, at electrode surfaces.

For initial study we selected electrode reactions involving simple one-electron transfer for which both redox states are detectably adsorbed and structurally similar. Although suitable model systems are not abundant, a number of Os(III)/(II) and Ru(III)/(II) pentaammine couples exhibit several desirable features. In particular, $Os(NH_3)_5L^{III/II}$ and $Ru(NH_3)_5L^{III/II}$ are substitutionally inert in both oxidation states for a number of coordinated ligands, L, which are also capable of binding to metal surfaces. Suitable bridging ligands include simple inorganic anions and organic ligands such as nitrogen heterocycles that contain an aromatic ring and/or a functional group expected to adsorb at silver. Suitably intense SER spectra were obtained for pentaammineruthenium(II) and pentaammineosmium(III) complexes containing pyridine (py) and pyrazine (pz), adsorbed at silver surfaces. Some spectra were also obtained for $Os^{III}(NH_3)_5bpy$ (bpy = 4,4′-bipyridine). Although the $Ru(NH_3)_5L^{III/II}$ couples have bulk-phase formal potentials, E_b^f, that are somewhat more positive (60 and 245 mV vs. SCE for L = py and pz, respectively[7a]) than the potential region (ca. 0 to −1.0 V vs. SCE) typically available at silver–aqueous interfaces, the corresponding $Os(NH_3)_5L^{III/II}$ couples have values of E_b^f that lie within this region (E_b^f = −650, −240, and −465 mV vs. SCE for L = py, pz, and bpy, respectively[7b,c]). The latter adsorbates are therefore expected to be present in either the III or II oxidation state at silver, depending on the applied potential. Alteration of the osmium oxidation state is expected to yield significant changes in the vibrational properties of the heterocyclic ring as well as in the metal–nitrogen modes since the added electron will be extensively delocalized via π-bonding. Such adsorbed redox couples having nitrogen heterocycle bridging groups constitute heterogeneous analogues of the much-studied intramolecular redox systems in homogeneous solution.[8] An additional reason for selecting these systems is that nitrogen heterocycles have received extensive scrutiny as model adsorbates for SERS at silver.[2]

(1) (a) Purdue University. (b) Graduate research assistant, Michigan State University, 1977–81. (c) Stanford University.

(2) For reviews, see: (a) Van Duyne, R. P. In "Chemical and Biochemical Applications of Lasers"; Moore, C. B., Ed.; Academic Press: New York, 1979; Vol. 4 Chapter 5. (b) Furtak, T. E.; Reyes, J. *Surf. Sci.* **1980**, *93*, 382. (c) Burke, R. L.; Lombardi, J. R.; Sanchez, L. A. *Adv. Chem. Ser.* **1982**, *201*, 69. (d) Chang, R. K.; Laube, B. L. *CRC Crit. Rev. Solid State Mater. Sci.*, in press. (e) Otto, A. In "Light Scattering in Solids"; Cardona, M., Guntherodt, G., Eds.; Springer: Berlin, 1984.

(3) (a) Weaver, M. J.; Barz, F.; Gordon, J. G., II; Philpott, M. R. *Surf. Sci.* **1983**, *125*, 409. (b) Hupp, J. T.; Larkin, D.; Weaver, M. J. *Surf. Sci.* **1983**, *125*, 429. (c) Weaver, M. J.; Hupp, J. T.; Barz, F.; Gordon, J. G., II; Philpott, M. R. *J. Electroanal. Chem.* **1984**, *160*, 321.

(4) (a) Barz, F.; Gordon, J. G., II; Philpott, M. R.; Weaver, M. J. *Chem. Phys. Lett.* **1982**, *91*, 291. (b) Philpott, M. R.; Barz, F.; Gordon, J. G., II; Weaver, M. J. *J. Electroanal. Chem.* **1983**, *150*, 399. (c) Barz, F.; Gordon, J. G., II; Philpott, M. R.; Weaver, M. J. *Chem. Phys. Lett.* **1983**, *94*, 168.

(5) (a) Farquharson, S.; Weaver, M. J.; Lay, P. A.; Magnuson, R. H.; Taube, H. *J. Am. Chem. Soc.* **1983**, *105*, 3350. (b) Taddayoni, M. A.; Farquharson, S.; Weaver, M. J. *J. Chem. Phys.* **1984**, *80*, 1363. (c) Taddayoni, M. A.; Farquharson, S.; Li, T. T-T.; Weaver, M. J. *J. Phys. Chem.*, in press. (d) Farquharson, S.; Milner, D.; Taddayoni, M. A.; Weaver, M. J. *J. Electroanal. Chem.*, in press.

(6) Guyer, K. L., Ph.D. Dissertation, Michigan State University, Lansing, MI, 1981.

(7) (a) Lim, H. S.; Barclay, D. J.; Anson, F. C. *Inorg. Chem.* **1972**, *11*, 1460. (b) Lay, P. A., unpublished results. (c) Sen, J.; Taube, H. *Acta Chem. Scand. Ser. A* **1979**, *A33*, 125.

(8) For example, see: Haim, A. *Prog. Inorg. Chem.* **1983**, *30*, 273.

0002-7863/84/1506-5123$01.50/0 © 1984 American Chemical Society

We present here SER spectra for these osmium and ruthenium complexes as a function of electrode potential. These are compared with corresponding vibrational spectra for the bulk-phase metal complexes in both III and II forms, along with electrochemical data for the adsorbed Os(III)/(II) couples, in order to explore the ability of SERS to detect redox transformations at metal surfaces. The potential-dependent surface concentrations of the Os(III) and Os(II) adsorbates as determined by using SERS are compared with corresponding data obtained by conventional electrochemical means. A preliminary communication describing SERS of adsorbed $Os(NH_3)_5py^{III/II}$ has already appeared.[5a] A complete compilation of the various vibrational bands, along with a detailed discussion of the vibrational mode assignments, is given elsewhere.[9]

Experimental Section

The various pentaammineruthenium(II) and pentaammineosmium-(III) complexes with pyridine, pyrazine, and 4,4′-bipyridine ligands were prepared as halide or trifluoromethanesulfonate salts essentially as detailed elsewhere.[10a,b] Both SERS and electrochemical studies employed 0.05–1 mM aqueous solutions in either 0.1 M NaCl or 0.1 M NaBr, which also contained 0.1 M HCl in the case of the pyridine complexes to suppress base-catalyzed disproportionation.[11] Ammine deuteration was performed by dissolving the complexes in neutral D_2O followed by acidification after ca. 5 min.

Raman excitation was obtained by using either a Spectra Physics Model 165 Kr^+ laser (647.1 nm) or Ar^+ laser (514.5 nm). Both a scanning double monochromator (either a Jarrell-Ash Model 25/100 or a SPEX 1403) and, later, a triple spectrograph optical multichannel analyzer (OMA) arrangement (SPEX 1877-PAR OMA 2) were utilized to obtain Raman spectra. Further details of the Raman and infrared experimental procedures are given in ref 9. The silver electrode was of rotating disk construction, having an exposed face of diameter 0.4 cm, encased by a Teflon shroud. It was mechanically polished successively with 1.0- and 0.3-μm alumina immediately before immersion in the cell. It was then electrochemically roughened in order to optimize the SERS intensities by means of an oxidation–reduction cycle (ORC) in the conventional manner,[2a] using a PAR 173 potentiostat with a PAR 179 digital coulometer. A typical ORC entailed stepping the potential from −150 to +250 mV and returning after the passage of 40 mC cm^{-2} of anodic charge. (This roughening procedure increases the actual silver surface area only ca. 2-fold.[3b]) The PAR 173 potentiostat was also used along with a PAR 175 potential programmer and a Houston 2000 X-Y recorder or a Nicolet 2090-1 digital oscilloscope to obtain cyclic voltammograms for both bulk solution and surface-bound redox couples. All experiments were conducted at 23 ± 1 °C and all electrode potentials are quoted with respect to the saturated calomel electrode (SCE).

Results

Electrochemistry of Adsorbed Os(III)/(II) Couples. Cathodic–anodic cyclic voltammetry of the $Os(NH_3)_5py^{III/II}$ couple at silver as well as at a hanging mercury electrode yielded a reversible wave with E_b^f = −650 mV in 0.1 M HCl. These voltammograms were obtained under conventional conditions (sweep rates ca. 100–500 mV s^{-1}, reactant concentration ca. 1 mM) for which the contribution from any initially adsorbed reactant is negligible. However, if the oxidized and reduced forms are sufficiently strongly adsorbed, the formal potential for the adsorbed redox couple can also be obtained by using cyclic voltammetry. This entails the use of sufficiently rapid sweep rates ($\gtrsim$20 V s^{-1}) and small bulk reactant concentrations ($\lesssim$0.1 mM) so that the faradaic current arises almost entirely from reaction of the initially adsorbed, rather than the diffusing, reactant. Figure 1A shows such a cyclic voltammogram for adsorbed $Os(NH_3)_5py^{III/II}$ at a roughened silver electrode in 0.1 M NaCl + 0.1 M HCl; the sweep rate was 200 V s^{-1}, and the bulk concentration, C_b, of $Os(NH_3)_5py^{3+}$ equaled 0.05 mM. The almost symmetrical shape and near coincidence of the cathodic and anodic peak potentials,

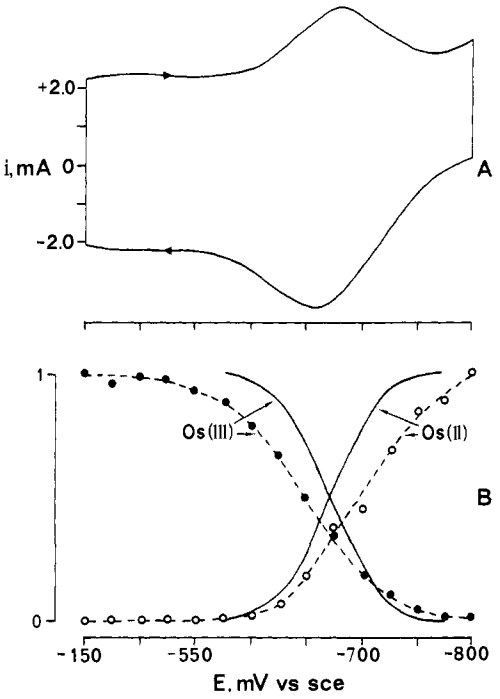

Figure 1. (A) Cathodic–anodic cyclic voltammogram for the adsorbed $Os(NH_3)_5py^{III/II}$ redox couple at roughened silver–aqueous interface in 0.1 M NaCl + 0.1 M HCl. Electrode (apparent area = 0.125 cm^2) roughened by means of an oxidation–reduction cycle in this supporting electrolyte (roughness factor ca. 1.8 on basis of capacitance measurements[3b]). Bulk $Os^{III}(NH_3)_5py$ concentration = 50 μM; sweep rate = 100 V s^{-1}. (B) Plots of relative surface concentrations for adsorbed $Os^{III}(NH_3)_5py$ and $Os^{II}(NH_3)_5py$ against electrode potential (solid curves), and relative peak intensities of the 1020- and 992-cm^{-1} SERS vibrational modes (dashed curves) plotted against electrode potential on the same scale. Experimental conditions as for Figure 1A. Solid lines were obtained by integrating the cyclic voltammogram in Figure 1A as outlined in the text. Both the adsorbate surface concentrations and the SERS intensities for Os(III) and Os(II) are those relative to the values at −150 and −800 mV vs. SCE (see text). SER spectra obtained by using 647.1-nm irradiation.

together with the observed linear dependence of the peak current upon sweep rate, indicate that the waves arise from initially adsorbed reactant. (The small separation between the cathodic and anodic peaks is probably due to uncompensated cell resistance.)

The formal potential for the adsorbed $Os(NH_3)_5py^{III/II}$ couple, E_a^f, is determined as 670 ± 5 mV from the position of the peak potentials. Reactant surface concentrations of 3–4 × 10^{-11} mol cm^{-2} (for C_b = 0.05 mM) were typically obtained from the faradaic charge contained under the voltammetric waves. The full width at half-peak height, $\Delta E_{p,1/2}$ = 95 mV, is close to the value, 91 mV, expected for a reversible adsorbed couple obeying the Langmuir isotherm.[12] Comparable results were also obtained for adsorbed $Os(NH_3)_5py^{III/II}$ in electrolytes containing 0.1 M NaBr (vide infra), with E_a^f = −700 mV and $\Delta E_{p,1/2}$ = 125 mV.

Similar measurements for solutions of $Os(NH_3)_5pz^{3+}$ in 0.1 M NaCl (pH 9) yielded somewhat less well-defined surface voltammograms, although a peak for adsorbed $Os(NH_3)_5pz^{III/II}$ was detected for C_b = 0.1 mM, corresponding to E_a^f = −335 mV (Figure 2A). More pronounced surface voltammograms were obtained for $Os(NH_3)_5bpy^{III/II}$ with E_a^f = −490 mV in 0.1 M NaCl (C_b = 50 μM). Although such voltammograms might conceivably be due to nonfaradaic (i.e., capacitive) rather than faradaic current, this is unlikely since no such peaks were detected in the absence of the adsorbate. The values of E_a^f in each case are not far from the values of E_b^f noted above for the corresponding bulk redox couples. The corresponding three ruthenium complexes yielded no detectable surface-bound redox couples within the

(9) Farquharson, S.; Lay, P. A.; Weaver, M. J. *Spectrochim. Acta A*, in press.

(10) (a) Ford, P.; Rudd, De F. P.; Gaunder, R.; Taube, H. *J. Am. Chem. Soc.* **1967**, *90*, 1187. (b) Lay, P. A.; Magnuson, R. H.; Sen, J.; Taube, H. *J. Am. Chem. Soc.* **1982**, *104*, 7658. (c) Magnuson, R. H.; Lay, P. A.; Taube, H. *J. Am. Chem. Soc.* **1983**, *105*, 2507.

(11) (a) Lay, P. A.; Magnuson, R. H.; Taube, H., to be published. (b) Rudd, D. P.; Taube, H. *Inorg. Chem.* **1971**, *10*, 1543.

(12) Bard, A. J.; Faulkner, L. R. "Electrochemical Methods"; Wiley: New York, 1980; p 522.

Table I. Major Vibrational Bands for Pentaamminepyridineosmium(III)/(II) at Silver Electrodes and in Bulk Media: Influences of Pyridine and Ammine Deuteration[m]

						surface-enhanced Raman[i]					
			N. Raman[d]	infrared[d]				pyridine-d_5[k]		ND_3[l]	
Wilson no.[a]	sym[b]	descript[c]	Os(III)[e]	Os(III)[e]	Os(II)[g]	−150 mV	−750 mV	−150 mV	−750 mV	−150 mV	−750 mV
	A_1	ν_{M-py}					267 s		263 m		256 s
	E	ν_{M-NH_3}				494 w	468 m	480 m	460 m,br	461 m,br	436 m
6a	A_1	δ_{ring}	654 m	649 w		654 m	648 s	623 w	618 m	655 m	647 m
11	B_2	γ_{C-H}	704 m	696 vs			739 w			701 m	698 w
10b	B_2	γ_{C-H}				895 w	900 m		702 m		898 w
1	A_1	ν_{ring}	1020 s	1022 m	990 m	1020 vs	992 s	978 vs	955 s	1019 vs	989 s
12	A_1	ν_{ring}		1074 s	1055 w	1076 m	1054 s	1042 m,sh	1025 m	1078 m	1054 m
9b,15	B_1	δ_{C-H}	1154 vw	1157 m		1151 w	1151 w				
9a	A_1	δ_{C-H}	1221 m	1216 m,br		1216 m,br	1210 s		896 m	1220 s	1210 s
14	B_1	δ_{C-H}		1373 s,sh		1386 s	1385 w	1322 vs	1325 m	1321 s	
19b	B_1	ν_{ring}		1442 vs		1441 w	1430 w,br			1443 w	
8a	A_1	δ_{ring}	1600 m,sh			1592 vs,br	1593 s	1552 vs	1550 s	1604 vs,br	1593 vs
	E	δ_{NH_3}(as)	1613 s	1608 vs		1620 s,br		1604 vs	1600 m,br	1170 s	
13	A_1	ν_{C-H}				2900 w,br	2910 w,br		2100 m,br		
7b	B_1	ν_{C-H}		2940 m						2930 s	2920 m,br

[a] As assigned for benzene: see ref 13. [b] Assuming C_{2v} symmetry for pyridine or pyrazine; C_{4v} symmetry for metal–nitrogen modes. [c] Vibrational assignments; see text and ref 9 for details. Symbols: ν, stretching mode; δ, in-plane bending mode; γ, out-of-plane bending mode. [d] Bulk Raman and infrared spectra recorded as mixture of Cl^-, ClO_4^-, I^-, or PF_6^- salt in KBr or CsI solid pellet. [e] Chloride salt. [f] Perchlorate salt. [g] Iodide salt. [h] Hexafluorophosphate salt. [i] SER spectra obtained by using ca. 0.1–1 mM complex at roughened silver electrode in either 0.1 M NaBr or 0.1 M NaCl (see text and figure captions for details). For pyridine complexes, electrolyte also contained 0.1 M HCl to suppress hydrolysis. Potentials quoted vs. saturated calomel electrode (SCE). [j] Obtained by using 0.01 M pyridine or pyrazine in 0.1 M NaCl. [k] SER spectra for complex prepared with pentadeuterated pyridine. [l] SER spectra for complex containing deuterated ammine ligands; prepared by dissolving complex in neutral D_2O. [m] Frequencies are given in cm^{-1} and are typically accurate to within 2–3 cm^{-1}. Explanation of symbols: w = weak, m = medium, s = strong, vs = very strong, br = broad, sh = shoulder. [n] Values in parentheses are frequencies for pyridine-deuterated complex.

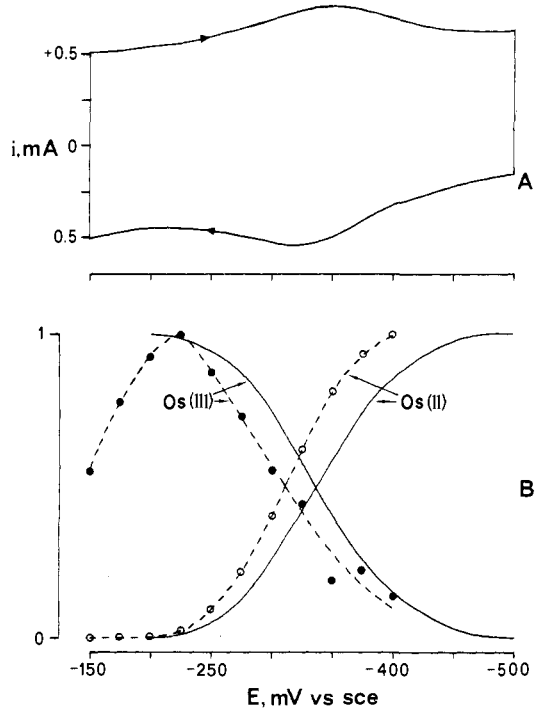

Figure 2. (A) Cathodic–anodic cyclic voltammogram for the adsorbed $Os(NH_3)_5pz^{III/II}$ redox couple at silver–aqueous interface. Conditions as in Figure 1A, except bulk Os(III) concentration = 100 μM, supporting electrolyte pH 9, sweep rate = 20 V s^{-1}. (B) Plots of relative surface concentrations for $Os^{III}(NH_3)_5pz$ and $Os^{II}(NH_3)_5pz$ against electrode potential (solid curves), and relative peak intensities of the 1093- and 1067-cm^{-1} SERS vibrational modes (dashed curves) plotted against electrode potential on the same scale. Experimental conditions as for Figure 2A. Solid lines were obtained by integrating the cyclic voltammogram in Figure 2A. SER spectra obtained by using 647.1-nm irradiation.

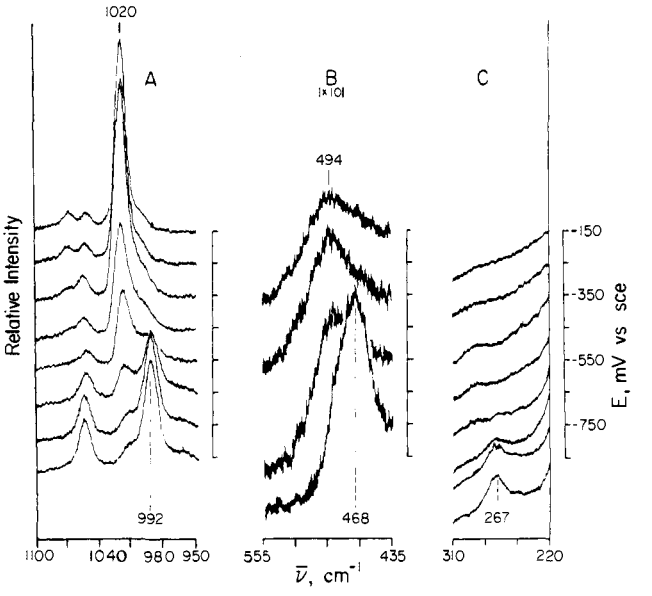

Figure 3. Representative SER spectra of $Os(NH_3)_5py$ as a function of electrode potential at roughened silver; solution contained 0.1 mM $Os(NH_3)_5py^{3+}$ in 0.1 M NaBr and 0.1 M HCl. Spectral conditions: 514.5-nm excitation, 100-mW incident power, 1-cm^{-1} s^{-1} scan speed, 1-s time constant, 4-cm^{-1} resolution. Spectra obtained at successively more negative potentials following surface roughening by means of an oxidation–reduction cycle (see text).

available potential range (0 to −1.0 V), as expected in view of the positive bulk formal potentials for these systems (vide supra).

SERS of $Os(NH_3)_5py$ and $Ru(NH_3)_5py$. Following an ORC at a roughened silver electrode in electrolytes containing either 0.1 M NaBr or 0.1 M NaCl, SER spectra were obtained for $Os(NH_3)_5py$ and $Ru(NH_3)_5py$ over the potential range −150 to −750 mV. (Note that metal oxidation states will be omitted when referring to the adsorbed complexes except for conditions where they are clearly known.) Representative spectra of $Os(NH_3)_5py$ and $Ru(NH_3)_5py$ for several key frequency regions are shown in Figures 3 and 4, respectively. Tabulations of the most important vibrational modes seen for these two systems at a representative pair of electrode potentials are given in Tables I and II. The pyridine ring modes are assigned Wilson numbers in accordance with established procedure.[13] These tables also contain summaries

(13) Lord, R. C.; Marton, A. L.; Miller, F. A. *Spectrochim. Acta* **1957**, *9*, 113.

Table II. Major Vibrational Bands for Pentaamminepyridineruthenium(III)/(II) at Silver Electrodes and in Bulk Media: Comparison with Pyridine[m]

			$Ru(NH_3)_5$pyridine						pyridine surface-enhanced Raman[j]	
			N. Raman[d]		infrared[d]		surface-enhanced Raman[i,n]			
Wilson no.[a]	sym[b]	descript[c]	Ru(III)[f]	Ru(II)[f]	Ru(III)[f]	Ru(II)[f]	−150 mV	−450 mV	−150 mV	−650 mV
	A_1	ν_{M-py}					303 vs	297 vs		
	E	ν_{M-NH_3}			482 m,sh	470 w				
6a	A_1	δ_{ring}	646 m	646 m	648 m	640 w	654 vs	655 s	625 w	627 w
11	B_2	γ_{C-H}			703 vs	693 m	683 s	682 m		
10b	B_2	γ_{C-H}			894 w				880 vw,br	875 vw,br
1	A_1	ν_{ring}	1023 s	1011 s	1017 s	998 s	1011 s	1012 s (977 s)	1007 vs	1006 s
12	A_1	ν_{ring}		1057 w	1069 s	1050 m	1054 s	1054 s (826 w)	1037 s	1034 s
15	B_1	δ_{C-H}			1153 m,sh	1150 w		1144 vw	1154 w	1153 vw
9a	A_1	δ_{C-H}	1218 s	1217 s	1223 m		1222 vs	1222 s (900 w)	1216 m	1216 m
14	B_1	δ_{C-H}			1393 s	1390 m				
19b	B_1	ν_{ring}			1446 vs	1446 s	1468 m	1468 m (1304 w)	1445 vw	
8a	A_1	δ_{C-H}	1606 s	1601 s		1604 s	1591 vs	1591 s (1564 s)	1597 m	1597 s
		δ_{NH_3}(as)		1611 vw	1609 vs	1610 s,br		(1609 s)		
7b	B_1	ν_{C-H}			2951 s,sh	2940 s,sh				

[a] For footnotes, see Table I.

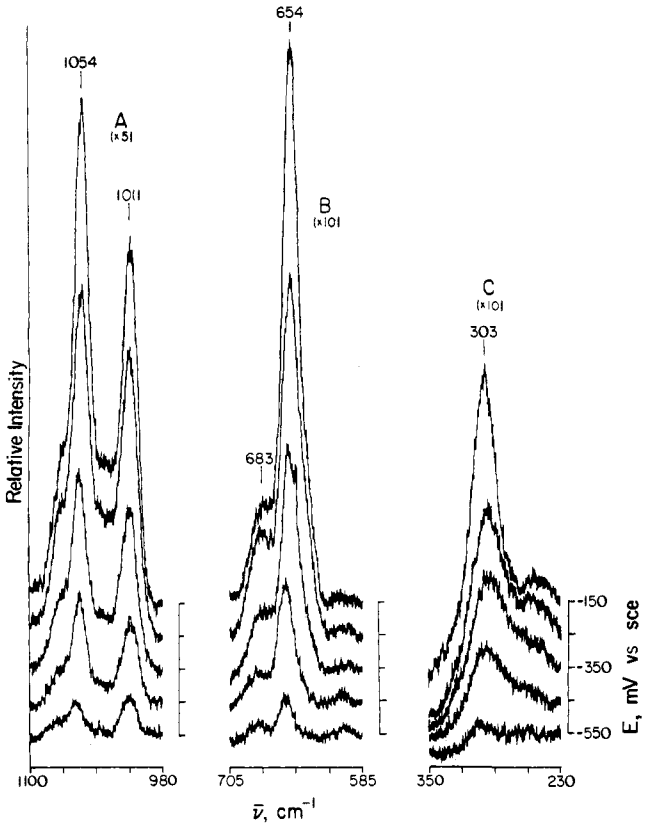

Figure 4. Representative SER spectra of $Ru(NH_3)_5$py as a function of electrode potential. Conditions as in Figure 3, except intensity scales differed from Figure 3A by factors indicated.

of the corresponding normal Raman and IR vibrational bands for the bulk-phase complexes in both III and II oxidation states. Table II additionally contains SERS data for pyridine obtained under similar conditions; the observed peak frequencies agree closely with previously detailed reports.[14,15] More complete tabulations of the Raman and IR spectra for these and the other complexes considered here, along with a more detailed discussion of the vibrational assignments, are given elsewhere.[9] The SER spectra were generally stable for at least 30–60 min using either 514.5- or 647.1-nm irradiation. However, significant intensity losses typically occurred at more negative potentials when using chloride rather than bromide electrolytes. The SER spectra could nonetheless be almost entirely regenerated by repolishing the electrode followed by another ORC.

The various mode assignments listed were made on the basis of group symmetry considerations, and by comparison of the relative frequencies and intensities with those for the Raman and IR spectra of uncoordinated pyridine[14-16] and a number of metal pyridine,[17] pyrazine,[18] and ammine[19] complexes for which detailed assignments are available. Although the normal Raman spectra of the bulk-phase complexes are too weak to detect all but the most prominent bands, the corresponding SERS spectra were sufficiently intense to exhibit these and most of the modes seen in the bulk-phase IR spectra.

A further aid to vibrational assignments for $Os(NH_3)_5$py was provided by examining the frequency shifts in the SER spectra brought about by separate deuteration of the pyridine ring or ammine hydrogens. The resulting peak frequencies are also included in Table I. SER spectra were also obtained for pyridine-deuterated $Ru(NH_3)_5$py; the peak frequencies obtained for this system are shown in parentheses in Table II. These frequency shifts enable a distinction to be made between vibrational modes associated chiefly with the ammine and pyridine ligands.[9] For example, the SERS peak at 468 cm^{-1} (−750 mV) shifts to a markedly lower frequency (436 cm^{-1}) upon ammine deuteration than that resulting from pyridine deuteration (461 cm^{-1}). This supports the assignment of this band to an osmium–ammine stretching mode. Indeed, the frequency ratio for the hydrogen to deuterium ammines (0.93) is close to the corresponding ratio (0.92) observed for ammine deuteration in $Ru(NH_3)_6^{3+}$.[19a] The strong bands seen at 267 cm^{-1} for $Os(NH_3)_5$py and at about 300 cm^{-1} for $Ru(NH_3)_5$py are assigned to a metal–pyridine stretching mode on the basis of the very similar frequencies observed for this mode in a number of other transition-metal pyridine complexes.[17] The slight frequency decreases seen for this band upon ammine deuteration (Table I) are consistent with coupling between the metal–pyridine and metal–ammine vibrations.

(14) Jeanmaire, D. L.; Van Duyne, R. P. *J. Electroanal. Chem.* **1977**, *84*, 1.

(15) Dornhaus, R.; Long, M. B.; Benner, R. E.; Chang, R. K. *Surf. Sci.* **1980**, *93*, 240.

(16) (a) Corrsin, L.; Fax, B. J.; Lord, R. C. *J. Chem. Phys.* **1953**, *21*, 1170. (b) Wilmshurst, J. K.; Bernstein, H. J. *Can. J. Chem.* **1957**, *35*, 1183.

(17) (a) Gill, N. S.; Nuttall, R. H.; Scaife, D. E.; Sharp, D. W. A. *J. Inorg. Nucl. Chem.* **1961**, *18*, 79. (b) Clark, R. J. H.; Williams, C. S. *Inorg. Chem.* **1965**, *4*, 350. (c) Choca, M.; Ferraro, J. R.; Nakamoto, K. *J. Chem. Soc., Dalton Trans* **1972**, 2297. (d) Akyiiz, S.; Dempster, A. B.; Morehouse, R. L.; Suzuki, S. *J. Mol. Struct.* **1973**, *17*, 105. (e) Flint, C. D.; Matthews, A. P. *Inorg. Chem.* **1975**, *14*, 1008.

(18) (a) Goldstein, M.; Unsworth, W. D. *Spectrochim. Acta* **1971**, *27A*, 1055. (b) Child, M. D.; Percy, G. C. *Spectrosc. Lett.* **1977**, *10*, 71. (c) Child, M. D.; Foulds, A. G.; Percy, G. C.; Thorton, D. A. *J. Mol. Struct.* **1981**, *75*, 191.

(19) (a) Senoff, C. V.; Allen, A. D. *Can. J. Chem.* **1967**, *45*, 1337. (b) Bee, M. W.; Kettle, S. F. A.; Powell, D. B. *Spectrochim. Acta* **1974**, *30A*, 139. (c) Schmidt, K. H.; Muller, A. *Inorg. Chem.* **1975**, *14*, 2183. *Coord. Chem. Rev.* **1976**, *19*, 41.

Table III. Major Vibrational Bands for Pentaamminepyrazineosmium(III)/(II) at Silver Electrodes and Bulk Media[m]

Wilson no.[a]	sym[b]	descript[c]	N. Raman Os(III)[e]	N. Raman Os(II)[e]	infrared Os(III)[e]	infrared Os(II)[g]	surface-enhanced Raman[i] −150 mV	surface-enhanced Raman[i] −550 mV	ND_3[l] −150 mV	ND_3[l] −550 mV
	A_1	ν_{M-pz}		287 s			345 vs	304 vs 343 s	345 vs	299 vs 340 s
	E	ν_{M-NH_3}				450 m	461 w	440 vw		
16b	B_{2u}	γ_{ring}					494 w	496 w	487 w	487 w
	A_g	δ_{ring}	710 s	707 s		700 s	702 s	673 vs 699 m	701 s	670 vs 700 m
4	3_g	γ_{C-H}					736 m	736 w		739 w
11	B_{2u}	γ_{ring}			816 w,sh		820 vw	814 w	816 w	807 m
1	A_g	ν_{ring}	1021 m	988 m	1022 m	1000 s	1020 s	985 m	1019 s	991 m
12	B_{1u}	ν_{ring}		1070 m	1090 w	1067 s	1095 m	1067 vs	1089 m	1066 vs
9a	A_g	δ_{C-H}	1236 m	1240 m	1251 m	1232 s	1232 s	1223 m	1230 s	1224 s
19b	B_{3u}	ν_{ring}			1441 m	1445 s	1464 m	1464 s	1464 s	1464 s
8a	A_g	ν_{ring}	1603 m	1601 s		1608 s,sh	1602 s	1590 m	1600 s	1594 s
		$\delta_{NH_3(as)}$	1614 w		1606 s,br	1616 s				

[a] For footnotes, see Table I.

The frequency shifts seen in the SER spectra for $Os(NH_3)_5py^{III/II}$ and $Ru^{II}(NH_3)_5py$ upon deuterating the pyridine ring are uniformly in good agreement with corresponding shifts seen both for bulk pyridine and several metal pyridine complexes.[17] Although most of the bands in the frequency region above ca. 600 cm^{-1} are associated with pyridine ring modes, there is also evidence for the appearance of internal ammine modes in the SER spectra. Thus, the strong NH_3 bending mode at 1620 cm^{-1} for $Os(NH_3)_5py$ (−150 mV) shifts to 1170 cm^{-1} upon ammine deuteration, similar to that observed for several metal ammine complexes.[19c]

Peaks at 240 and 180 cm^{-1} were also observed in chloride and bromide electrolytes, respectively. Since very similar bands are also observed in pure halide electrolytes[3c,20] and the pyridine complexes lack an electron lone pair for surface binding, they are attributed to surface-halide stretching modes. All the adsorbate vibrational bands occurred at essentially identical frequencies in chloride- and bromide-containing electrolytes. However, the latter medium was employed for most measurements since it yielded more stable SER spectra, especially at more negative potentials.

The SER spectra for $Os(NH_3)_5py$ and $Ru(NH_3)_5py$ exhibit two significant differences as the potential is made progressively more negative. Firstly, the signal intensity for the latter system decreases to a markedly greater extent than for the former. Secondly, several peaks in the $Os(NH_3)_5py$ spectrum disappear, being replaced by peaks at lower frequencies. In particular, the osmium–ammine stretch at 494 cm^{-1} and the symmetric ring-breathing mode at 1020 cm^{-1}, both present within the potential region ca. −100 to −600 mV, are replaced at more negative potentials by peaks at 468 and 992 cm^{-1}, respectively (Figure 3). A peak at 267 cm^{-1}, tentatively assigned to a metal–pyridine mode,[9] also appears at more negative potentials (Figure 3).[21] Such a frequency decrease for the metal–ammine mode is consistent with a reduction of Os(III) to Os(II) (vide infra).[19] The frequency shift for the symmetric ring-breathing mode (Wilson mode 1) corresponds closely to the frequency difference seen in the IR spectra of $Os^{III}(NH_3)_5py$ and $Os^{II}(NH_3)_5py$ (Table I). A sufficiently pure sample of $Os^{II}(NH_3)_5py$ could not be obtained to allow the corresponding frequency shifts for the other modes to be determined. However, a comparison with the corresponding spectral differences between bulk-phase $Ru^{III}(NH_3)_5py$ and $Ru^{II}(NH_3)_5py$ (Table II) indicates that the frequency shifts seen for other modes in the SER spectra of $Os(NH_3)_5py$ beyond ca. −600 mV are also consistent with a decrease in metal oxidation state. Several other SERS bands for $Os^{III}(NH_3)_5py$ also exhibit significant frequency shifts upon reduction to Os(II). In particular, the asymmetric ring breathing mode shifts from 1076 to 1054 cm^{-1} and the symmetric N–H bending mode from 1354 to 1254 cm^{-1} (Table I).

The relative peak intensities of the 1020- and 992-cm^{-1} SERS vibrational modes of $Os(NH_3)_5py$, I_{III}^P and I_{II}^P, respectively, are plotted (dashed lines) as a function of electrode potential in Figure 1B. (The potential-dependent spectra used to construct Figure 1B were obtained by using the optical multichannel analyzer to minimize errors arising from the temporal decay of the Raman signals.[5c]) The intensities are normalized to the values seen at the potentials, ca. −450 and −800 mV, for the 1020- and 992-cm^{-1} modes, respectively. These potentials span the region within which one band is replaced entirely by the other. For comparison, corresponding plots of the relative surface concentrations of $Os(NH_3)_5py^{III}$ and $Os(NH_3)_5py^{II}$, Γ_{III} and Γ_{II}, respectively, are shown as solid curves in Figure 1B. These were obtained by integrating the cyclic voltammogram in Figure 1A to yield faradaic charge–potential (q_f–E) plots, from which the normalized Γ–E plots were obtained directly since $q_f \propto \Gamma$. (Note that Γ_{III} and Γ_{II} are related by $\Gamma_{III} = 1 - \Gamma_{II}$.) Formal potentials for the adsorbed Os(III)/(II) couple may conveniently be obtained from the intersection of the corresponding Os(III)–E and Os(II)–E curves. That determined from SERS, $E_{SER}^f = -670 \pm 10$ mV, is identical with the cyclic voltammetric value, E_a^f (vide supra). (This supplants the earlier reported value[5a] of −630 mV, obtained by using a scanning spectrometer.) Corresponding SERS data gathered in bromide electrolytes yielded similar results, with $E_{SERS}^f \approx E_a^f$.

SERS of $Os(NH_3)_5pz$ and $Ru(NH_3)_5pz$. Relative Raman Intensities. SER spectra were recorded for solutions containing ca. 0.1 mM $Os(NH_3)_5pz^{3+}$ and $Ru(NH_3)_5pz^{2+}$ in 0.1 M NaCl or 0.1 M NaBr as a function of electrode potential under similar conditions to those employed for the pyridine complexes. Representative spectra for some key frequency regions are shown for $Os(NH_3)_5pz$ and $Ru(NH_3)_5pz$ in Figures 5 and 6, respectively. The various vibrational bands observed for these systems are summarized in Tables III and IV, together with the corresponding bands obtained for SERS of pyrazine obtained under similar conditions and normal Raman and IR spectra of the bulk complexes in III and II oxidation states. The vibrational assignments given in these tables are based partly on comparisons with those given previously for pyrazine[13,15] and for bulk-phase metal pyrazine complexes.[18]

Several features of these SER spectra are worthy of particular comment. Firstly, most vibrational bands associated with ring modes in both the $Os(NH_3)_5pz$ and $Ru(NH_3)_5pz$ SER spectra are 10- to 50-fold more intense than in the SER spectra for the corresponding pyridine complexes. Secondly, in contrast to the behavior of the corresponding pyridine complexes, most bands in the $Os(NH_3)_5pz$ spectra become more intense as the potential is made more negative. The intensity of the $Ru(NH_3)_5pz$ spectra is only mildly potential dependent (Figures 5 and 6). Thirdly,

(20) For example, see: Wetzel, H.; Gerischer, H.; Pettinger, B. *Chem. Phys. Lett.* **1981**, *78*, 392.

(21) We previously attributed a weak band found at 291 cm^{-1} for $Os(NH_3)_5py$ at less negative potentials to an Os(III)–py stretching mode.[5a] However, this assignment is inconsistent with that for Os(II)–py stretching at 267 cm^{-1} in view of the *decrease* in the metal–pyridine bond length upon Os(III) reduction expected from the known behavior of the corresponding Ru(III)/(II) couple. See: Gress, M. E.; Creutz, C.; Quicksall, C. O. *Inorg. Chem.* **1981**, *20*, 1522.

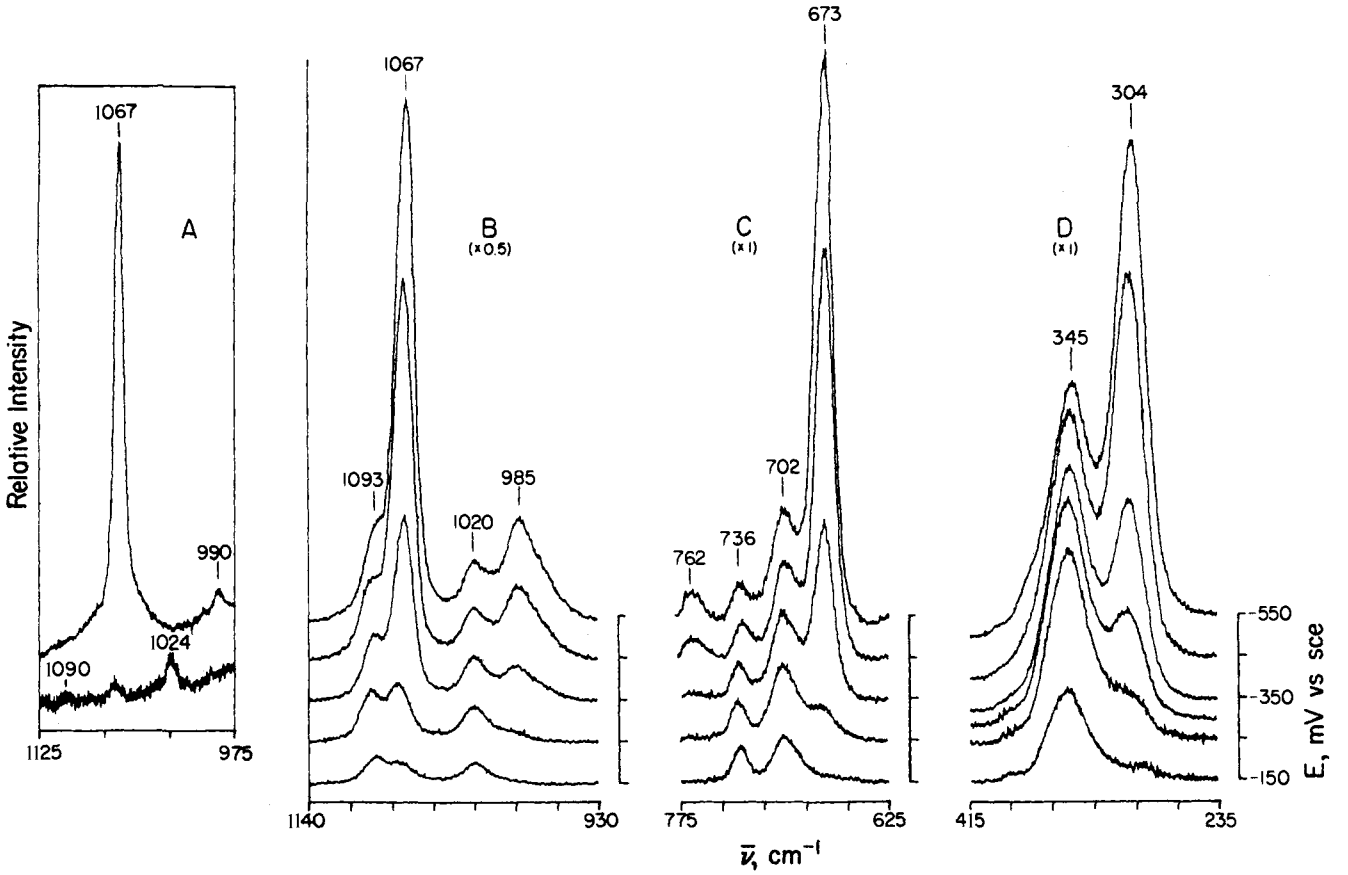

Figure 5. (A) Solution Raman spectrum of $Os^{III}(NH_3)_5pz$ (lower trace) and of $Os^{II}(NH_3)_5pz$ (upper trace, ×0.5). Sample concentration = 2.5 mM. Conditions as in Figure 3, except incident laser power was 400 mW. (B–D) Representative SER spectra of $Os(NH_3)_5pz$ as a function of electrode potential. Conditions as in Figure 3, except supporting electrolyte was 0.1 M NaCl and intensity scales differed from Figure 3A by factors indicated.

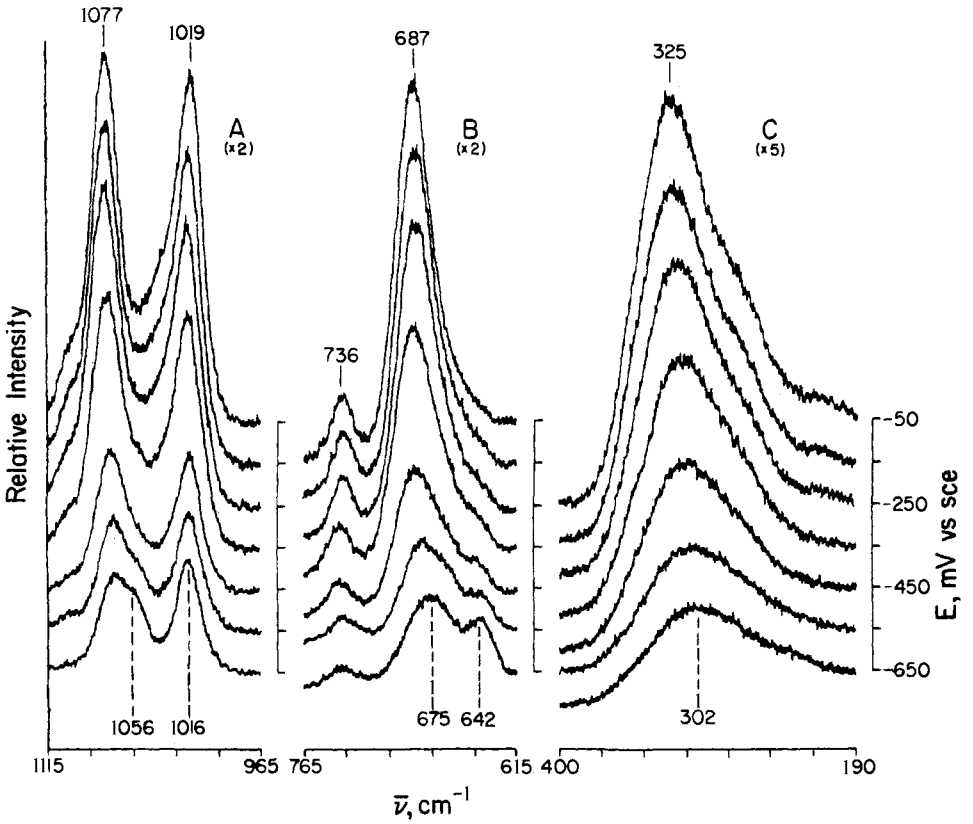

Figure 6. Representative SER spectra of $Ru(NH_3)_5pz$ as a function of electrode potential. Conditions as in Figure 3, except supporting electrolyte was 0.1 M NaCl + 10^{-4} M HCl and intensity scales differed from Figure 3A by factors indicated.

Table IV. Major Vibrational Bands for Pentaamminepyrazineruthenium(III)/(II) at Silver Electrodes and in Bulk media: Comparison with Pyrazine[m]

Wilson no.[a]	sym[b]	descript[c]	$Ru(NH_3)_5$pyrazine N. Raman[d] Ru(II)[h]	$Ru(NH_3)_5$pyrazine infrared[d] Ru(II)[h]	$Ru(NH_3)_5$pyrazine surface-enhanced Raman −150 mV	$Ru(NH_3)_5$pyrazine surface-enhanced Raman −650 mV	pyrazine surface-enhanced Raman[j] −150 mV	pyrazine surface-enhanced Raman[j] −650 mV
	A_1	ν_{M-pz}	315 m,br		325 s,br	302 s,br		
	E	ν_{M-NH_3}	451 vs	456 w	455 vw			
6a	A_g	δ_{ring}	692 m		687 s	675 s	639 s	636 s
4	B_{3g}	γ_{C-H}			736 m	735 m	699 m	699 m
10a	B_{1g}	γ_{C-H}		753 sh,br			742 m	744 m
11	B_{2u}	γ_{C-H}			820 m	819 m	806 m	812 m,br
1	A_g	ν_{ring}	1019 m	1013 m	1019 s	1016 s	1020 s	1021 s
12	B_{1u}	ν_{ring}	1076 m,br		1077 s	1056 m,sh 1074 m	1088 m	
9a	A_g	δ_{C-H}	1229 s	1221 s	1227 vs	1223 s	1225 s	1225 s
19b	B_{3u}	ν_{ring}		1467 m	1472 m	1471 m	1464 w	1467 w
19a	B_{1u}	ν_{ring}		1480 m			1479 w	1479 w
8a	A_g	ν_{ring}	1601 s	1579 s	1593 vs	1591 s	1590 vs	1588 vs
		$\delta_{NH_3(as)}$		1620 s,br				

[a] For footnotes, see Table I.

the SER spectral features seen in the 150–400-cm^{-1} region for both $Os(NH_3)_5pz$ and $Ru(NH_3)_5pz$ differ markedly from those seen for either the corresponding bulk spectra or the SER spectra for the pyridine complexes. Thus, $Os(NH_3)_5pz$ exhibits intense peaks at 304 and 345 cm^{-1} (Figure 5) whereas $Ru(NH_3)_5pz$ yields a single broad peak around 300–325 cm^{-1}, the frequency depending on the potential (Figure 6).

The potential-dependent SER spectra for $Os(NH_3)_5pz$ (Figure 5) are in some respects similar to those for $Os(NH_3)_5py$. Thus, bands appear at both 1020 and 985 cm^{-1}, which as for the pyridine analogue can be assigned to the symmetric ring breathing modes in Os(III) and Os(II), respectively, on the basis of the frequencies in the bulk-phase spectra (Table III). However, unlike $Os(NH_3)_5py$ there is no straightforward potential-dependent substitution of Os(III) by the corresponding Os(II) bands. Instead, altering the potential to more negative values in the vicinity of E_a^f (−335 mV, vide supra) yields a dramatic increase in the intensity of several $Os(NH_3)_5pz$ bands associated with Os(II) (particularly those at 673, 985, and 1067 cm^{-1}, Figure 5). This occurs without a sizable decrease in some bands expected to be associated with Os(III), especially that at 1020 cm^{-1}. Nevertheless, these results may be rationalized by referring to the corresponding solution Raman spectra for 2.5 mM $Os(NH_3)_5pz^{3+}$ and $Os(NH_3)_5pz^{2+}$, a segment of which is also shown in Figure 5. The normal Raman Os(II) bands are substantially more intense than those for Os(III). In particular, the intensity of mode 12 for Os(II) (1067 cm^{-1}) increases dramatically relative to that for the Os(III) form (1090 cm^{-1}).

With this in mind, a plot of the potential-dependent peak intensities of the 1093- and 1067-cm^{-1} bands in the $Os(NH_3)_5pz$ SER spectra was prepared (cf. Figure 1B); this is shown in Figure 2B. As in Figure 1B, the SERS data are compared with the Os(III)/(II) surface-redox behavior determined from rapid cyclic voltammetry (Figure 2A). Although the latter band is considerably more intense, once normalized to their values at potentials spanning the potential-dependent region (ca. −200 to −450 mV) reasonable correspondence between the Os(III)/(II) redox behavior sensed by SERS and conventional electrochemistry is again obtained. Thus, the formal potential determined from SERS, $E_{SER}^f = -310 \pm 10$ mV, is close to the voltammetric value, $E_a^f = -335$ mV (vide supra).

The survival of several bands at first sight due to $Os(NH_3)_5pz^{3+}$, especially those at 1020, 702, and 345 cm^{-1} (Figure 5), even at potentials negative of this region is nevertheless puzzling. The band at 1020 cm^{-1}, at least, may be ascribed to adsorbed pyrazine, presumably present as an impurity.

The relative Raman scattering efficiencies for the complexes as well as for uncoordinated pyridine and pyrazine were determined both in aqueous solution and at the electrode surface. The latter utilized coverage data determined for the complexes as above and for the free ligands from capacitance–potential measurements.[22] Although detailed data will be given elsewhere,[23] some results pertinent to the present study are now summarized. The internal heterocyclic modes in the solution-phase Raman spectra of the pyridine and pyrazine complexes were substantially (up to 10^3-fold) more intense than for the free ligands using 647-nm and especially 514.5-nm irradiation. This is indicative of electronic resonance enhancement, as might be expected in view of the proximity of the irradiation wavelengths to intense electronic adsorption bands for these complexes.[7c,10] Comparably larger intensities were typically also seen in the SER spectra of the complexes relative to those for the absorbed ligands. Consequently, the surface enhancement factors (SEF) for these systems, i.e., the Raman scattering efficiency of the adsorbed relative to the corresponding bulk-phase species, are not greatly different, lying in the range ca. $1-10 \times 10^6$ (cf. ref 2a). Nonetheless, some significant variations in SEF were observed. Especially large SEF were determined for $Os(NH_3)_5pz$, which are somewhat dependent on the laser excitation wavelength. Thus, for mode 12 of $Os(NH_3)_5pz^{2+}$ (1067 cm^{-1}) at 514.5 nm, SEF $\approx 5.5 \times 10^6$, whereas at 647 nm, SEF $\approx 2.5 \times 10^8$.[23]

SERS of $Os(NH_3)_5$bpy. Although the vibrational spectra of bipyridine complexes are rather more complicated than for single-ring heterocycles, the appearance of a well-defined adsorbed $Os(NH_3)_5bpy^{III/II}$ couple from cyclic voltammetry (vide supra) prompted us to examine SERS of $Os(NH_3)_5$bpy as a function of electrode potential (Figure 7). A tabulation of the SER spectral bands along with vibrational assignments is given in ref 9. Although alteration of the electrode potential to values negative of the formal potential for the adsorbed Os(III)/(II) couple (−490 mV, vide supra) yielded little change for most vibrational modes, the symmetric ring breathing mode at 1005 cm^{-1} decreased in intensity, and a new band at 996 cm^{-1} appeared. By analogy with the results for the $Os(NH_3)_5py^{III/II}$ couple noted above, this may be associated with the formation of Os(II) from Os(III). However, this conclusion is tempered by the greater uncertainty in assigning such bands in view of the relatively complicated structure of the adsorbate.

Discussion

Since the silver electrode is composed of an array of surface sites having subtly different structural properties, and given that only a minority of these sites may contribute predominantly to SERS,[2] it is of central interest to compare the energetics of such "Raman-active" sites as measured by the potential-dependent Raman intensities with that for the overall surface as obtained from conventional electrochemistry.[3] The remarkable similarity in the potential dependence of the relative surface concentrations of $Os^{III}(NH_3)_5py$ and $Os^{II}(NH_3)_5py$, Γ_{III} and Γ_{II}, with the cor-

(22) Gennett, T.; Weaver, M. J., unpublished results.
(23) Farquharson, S.; Taddayoni, M. A.; Weaver, M. J., in preparation.

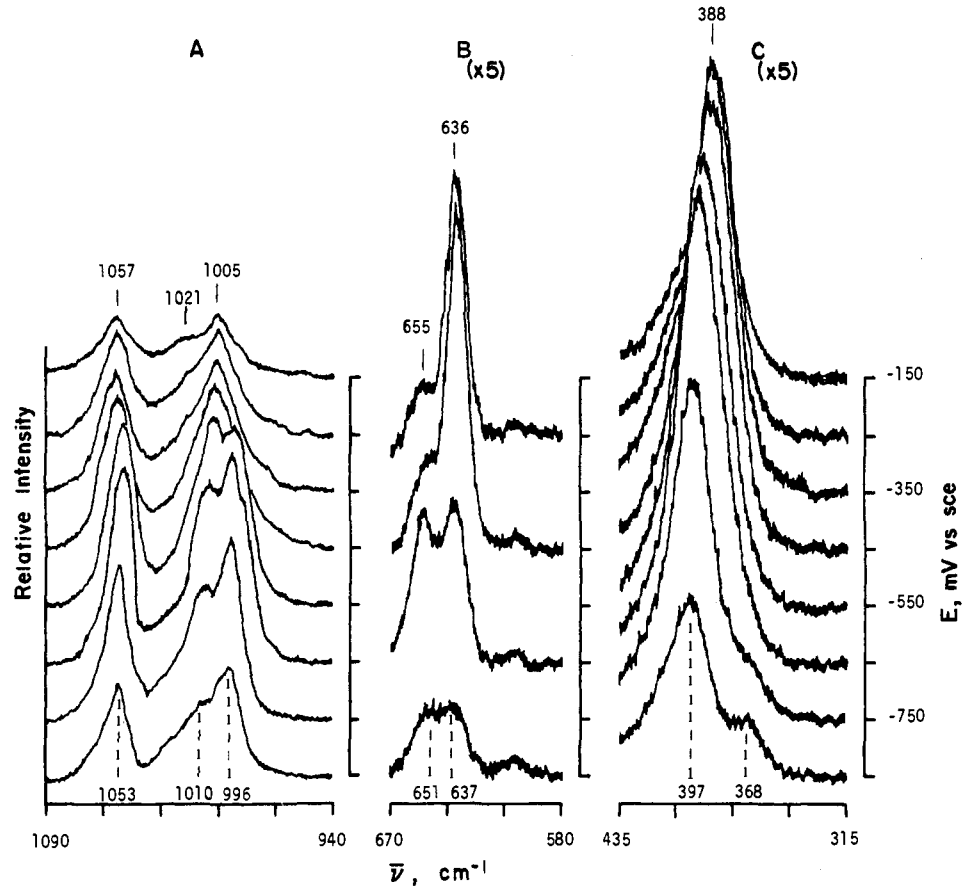

Figure 7. Representative SER spectra of $Os(NH_3)_5bpy$ as a function of electrode potential. Conditions as in footnote to Figure 6.

responding relative intensities of the symmetric ring modes, I_{III}^{P} and I_{II}^{P} (Figure 1B), so that $E_a^f \approx E_{SER}^f$, indicates that the redox properties of the surface sites that are responsible for the observed Raman signals do not differ significantly from those for the sites occupied by the majority of the adsorbate. The same conclusion applies to the $Os(NH_3)_5pz^{III/II}$ couple (Figure 2B), albeit with less certainty given the less straightforward nature of the Os(III)/(II) SERS behavior for this system.

As noted previously,[5a] the observation of SERS for the pyridine complexes is of significance in itself since no unshared electron pairs are available on the pyridine or ammine ligands with which to form an adsorbate–surface bond. Such bonding is commonly considered to be a desirable or even required feature for SERS.[2e] However, *N*-methylpyridinium has been shown to yield SERS at silver in the presence of adsorbed iodide,[24] and SERS have also been observed for $Ru^{III}(2,2'\text{-bpy})_3$ and related complexes.[25] Most strikingly, we have recently demonstrated that SERS can be obtained for transition-metal hexaamine cations at silver in the presence of adsorbed halide, even though such species clearly cannot interact specifically with the electrode surface.[5b] One such electroactive system, $Ru(NH_3)_6^{3+/2+}$, also yields a value of E_{SER}^f almost identical with that of E_a^f, measured here by means of rapid cyclic voltammetry.[5b] In common with the present adsorbed $Os(NH_3)_5py^{3+/2+}$ and $Os(NH_3)_5pz^{3+/2+}$ couples, $Ru(NH_3)_6^{3+/2+}$ exhibits a value of E_a^f that is somewhat (20–100 mV) more negative of that for the solution-phase couple, E_b^f, in both chloride and bromide media. This shift is consistent with the expected double-layer potentials at the adsorption site, ϕ_R, generated by the extensive halide adsorption occurring at silver in this potential region (−200 to −700 mV).[3b] Thus, on the basis of simple electrostatics, it is expected that $E_a^f = E_b^f + \phi_R$. Electrostatic double-layer attraction, clearly all-important for $Ru(NH_3)_6^{3+/2+}$, therefore appears also to be a crucial factor in generating the high interfacial concentrations (i.e., strong adsorption) seen for the present Os(III)/(II) couples in chloride or bromide media.

The possible surface orientations are restricted for the adsorbed pyridine complexes; inspection of molecular models shows that the ammine ligands will prevent the pyridine ring from lying flat on the electrode surface. These complexes may adsorb with the ring on edge,[26] oriented so to enable osmium or ruthenium to ion pair with the coadsorbed bromide or chloride anions. Indeed, the halide ions play an important role in stabilizing the SERS signals. This is evidenced by the decreases in SERS intensity, especially for $Ru^{II}(NH_3)_5py$, brought about by altering the potential to more negative values where the halide coverage decreases (Figure 3),[3b,c] as indicated by the disappearance of the surface-halide stretching bands. Also worthy of comment is the appearance of SERS bands associated with metal–ammine and internal ammine modes in addition to metal–pyridine and internal pyridine modes (Tables I, II), even though the coupling between the ammine ligands and the electrode surface must be extremely weak (cf. ref 5b). Indeed, the intensities of the internal ammine modes relative to the nitrogen heterocycle modes are not substantially different in the SER and normal Raman spectra. All these findings clearly indicate that strong adsorbate–surface interactions are not a prerequisite for the observation of intense SERS.

A previous comparison of the bulk vibrational spectra of liquid pyridine with a number of divalent metal–pyridine complexes has shown that the frequency of a number of pyridine ring modes, especially modes 6a (605 cm^{-1}), 1 (990 cm^{-1}), and 8a (1590 cm^{-1}), increases significantly upon coordination.[17d] These shifts can be ascribed in part to coupling with low-frequency metal–pyridine vibrations.[17d] Similarly, the frequencies of most pyridine modes in the SER spectra of $Os^{III}(NH_3)_5py$, $Os^{II}(NH_3)_5py$, and Ru^{II}-

(24) Bunding, K. A.; Bell, M. I.; Durst, R. A. *Chem. Phys. Lett.* **1982**, *89*, 54.

(25) Buck, R. P.; Chambers, J. A. *J. Electroanal. Chem.* **1982**, *140*, 173. Stacy, A. M.; Van Duyne, R. P. *Chem. Phys. Lett.* **1983**, *102*, 365.

(26) Conway, B. E.; Mathieson, J. G.; Dhar, H. P. *J. Phys. Chem.* **1974**, *78*, 1226.

$(NH_3)_5py$ are close to, but significantly higher than, those for the corresponding bands in the SER spectra for free pyridine; a few modes, most notably the A_1 δ_{ring} mode (6a), exhibit 20–30-cm^{-1} higher frequencies in the metal complexes (Tables I, II). The close similarities in the frequencies of all modes in the SER spectra of these complexes with those in the corresponding bulk-phase spectra (Tables I, II) indicate that the silver surface exerts only a very minor perturbation on the bonding within these complexes.

The notably (10–30 cm^{-1}) lower frequencies of several metal–ligand and pyridine ring modes for $Os^{II}(NH_3)_5py$ compared with $Os^{III}(NH_3)_5py$ (Table I) are consistent with the high degree of metal-to-ligand back-bonding expected for Os(II), yielding an increase of π electron density on the pyridine ring for $Os^{II}(NH_3)_5py$ compared to $Os^{III}(NH_3)_5py$. Interestingly, the frequency of the symmetric ring breathing mode for $Os^{II}(NH_3)_5py$ (992 cm^{-1}) is noticably lower than for $Ru^{II}(NH_3)_5py$ (1012 cm^{-1}). This mode is known to be especially sensitive to the pyridine environment.[27] This lower value of ν_{ring} for $Os^{II}(NH_3)_5py$ is consistent with the more extensive metal-to-ligand back-bonding expected for Os(II) than for Ru(II)[28] and suggests that the force constant of the ring mode is decreased as a result of a greater non-bonding electron density.

The comparison between the SER spectra of the pyrazine and pyridine complexes is interesting since, unlike the latter, surface binding for the former complexes can occur via the remote pyrazine nitrogen. By analogy with the known influence of coordination at the remote nitrogen upon the redox behavior of $Os(NH_3)_5pz^{III/II}$,[10b,c] surface attachment via this nitrogen might be expected to yield large ($\gtrsim$200 mV) positive shifts in E_a^f resulting from stabilization of the Os(II) state. However, as noted above, both the SERS and electrochemical data for $Os(NH_3)_5pz$ (Figures 2 and 5) yield a formal potential, $E_a^f \sim -320$ mV, that is distinctly *negative* of that for the bulk couple, −240 mV. It is conceivable that a portion of the Os(II) adsorbate is sufficiently stabilized with respect to electrooxidation that it is effectively electroinactive at silver; however, this is inconsistent with the loss of the Os(II) SER signals positive of ca. −300 mV. This therefore suggests that nitrogen surface coordination of $Os(NH_3)_5pz$ does not exert a major influence upon the redox behavior.

Nevertheless, some spectral features for the pyrazine complexes suggest that adsorbate–surface electronic coupling plays a more significant role than for the pyridine complexes. The appearance of especially intense bands around 300 cm^{-1} in the SER spectra of both $Os(NH_3)_5pz$ and $Ru(NH_3)_5pz$, attributed to metal–pyrazine stretching modes,[9] is of interest in this regard. The breadth of the $Ru(NH_3)_5pz$ band together with its potential dependence (Figure 6) suggests that it is composed of more than one vibrational mode; indeed, two distinct bands are seen for $Os(NH_3)_5pz$ (Figure 5). These bands may well correspond to metal–pyrazine vibrations at different surface sites.

The especially large SEF seen for adsorbed $Os(NH_3)_5pz^{2+}$ at 647.1 nm excitation suggests that significant modifications in the electronic properties are brought about by adsorption. Raman excitation profile measurements, presented elsewhere,[23] indicate that the prominent electronic adsorption band, centered at 460 nm,[7c] for bulk $Os(NH_3)_5pz^{2+}$, is noticeably red shifted for the adsorbed species. This yields further SERS enhancements for excitation wavelengths, such as 647.1 nm, that are in the long-wavelength "tail" of the absorption band.

The differences in the potential dependencies of the overall SERS intensities for the pyridine and pyrazine complexes is also suggestive of nitrogen surface binding for the latter. As noted above, the appearance of SERS for the former adsorbates appears to require strong halide coadsorption. In contrast, SERS for the pyrazine complexes persists even at the most negative potentials (ca.−750 mV) where halide coadsorption is relatively weak. Presumably the nitrogen-bound pyrazine complexes can both create and stabilize "Raman-active" sites, whereas the surface sites responsible for SERS of pyridine complexes are both created and stabilized by surrounding halide anions.

The near-zero separation of the cathodic and anodic peak potentials for the adsorbed $Os(NH_3)_5py^{III/II}$ redox couple (Figure 1A) indicates that the heterogeneous electron-transfer reaction is rapid on the electrochemical time scale ($\gtrsim 10^{-3}$ s). However, the presence of distinct vibrational modes associated with Os(III) and Os(II) indicates that it is a valence-trapped (class II) system[29] on the vibrational time scale. This is expected in view of the relatively weak coupling between the osmium redox center and the metal surface for this system. The SERS of $Os(NH_3)_5pz^{III/II}$ also shows hallmarks of class II behavior (cf. mixed-valence diruthenium complexes[30]).

Concluding Remarks

The foregoing demonstrates that SERS can provide a valuable tool for examining sequential redox states for adsorbed coordination compounds at metal surfaces. Particularly encouraging is the remarkably close correspondence between the potential-dependent redox equilibria for adsorbed transition-metal couples as sensed by SERS and those obtained from conventional electrochemistry and the simple rationalization of the adsorption-induced changes in the redox equilibria in terms of electrostatic double-layer effects. It also suggests that SERS can usefully be employed to unravel redox pathways for more complex electrochemical reactions involving adsorbed species where the identification of the intermediates and products can be fraught with difficulties.

In view of the intensity and richness of the SER spectra, the technique shows promise as a means of obtaining hitherto unavailable vibrational information for coordination compounds that can be electrostatically or chemically bound to silver electrodes. This includes oxidation states, such as Os(II), that are difficult to obtain in pure form in bulk media due to their chemical reactivity. Such information for sequential oxidation states is required in order to understand redox reactivity in terms of the molecular structural changes accompanying electron transfer. This approach also enables information to be gained for the first time on the molecular details associated with heterogeneous electron-transfer processes. Measurements of the dynamic as well as equilibrium properties of transition-metal adsorbates obtained by using time-resolved SERS combined with conventional electrochemistry are under way in our laboratory.

Acknowledgment. The electrochemical measurements were performed by Joseph Hupp. We thank George Leroi for the use of a Raman spectrometer. The synthesis and characterization of the osmium complexes were performed in the laboratory of Henry Taube at Stanford University. We also thank Henry Taube for his advice and encouragement. The research program of M.J.W. is supported in part by the Office of Naval Research and the Air Force Office of Scientific Research and the research program of H.T. by the NSF (Grant CHE 79-08633) and NIH (Grant GM 13638-17). P.A.L. acknowledges a CSIRO Postdoctoral Fellowship, and M.J.W. a Sloan Foundation Fellowship.

Registry No. $Os(NH_3)_5py^{3+}$, 83781-38-8; $Os(NH_3)_2pz^{3+}$, 83781-34-4; $Os(NH_3)_5bpy^{3+}$, 91002-49-2; $Ru(NH_3)_5py^{2+}$, 21360-09-8; $Ru(NH_3)_5pz^{2+}$, 19471-65-9; $Ru(NH_3)_5bpy^{2+}$, 54714-01-1; Ag, 7740-22-4.

(27) Hendra, P. J.; Horder, J. R.; Loader, E. J. *J. Chem. Soc. A* **1971**, 1766.

(28) This follows from the greater overlap expected between the osmium 5d non-bonding orbitals and ligand π-orbitals than that expected for the less extended ruthenium 4d orbitals.

(29) Robin, M. B.; Day, P. *Adv. Inorg. Chem. Radiochem.* **1967**, *10*, 247.

(30) Creutz, C. *Prog. Inorg. Chem.* **1983**, *30*, 1.